Remote ion temperature measurements of Earth's magnetosphere: Medium energy neutral atom (MENA) images

E. E. Scime,[1] A. M. Keesee,[1] J.-M. Jahn,[2] J. L. Kline,[1] C. J. Pollock,[2] and M. Thomsen[3]

Received 27 August 2001; revised 18 February 2002; accepted 19 February 2002; published 28 May 2002.

[1] Energy spectra of ENA images obtained with the MENA imager on the IMAGE observatory are used to construct remote images of the plasma ion temperature. The remotely measured ion temperatures are consistent with in-situ ion temperature measurements. During the storm of August 12, 2000, the ion temperatures on the dawn side of the magnetosphere are significantly lower than the dusk side ion temperatures. Similar observations of ion temperature asymmetry are presented for three other storm periods. *INDEX TERMS:* 2730 Magnetospheric Physics: Magnetosphere–inner; 2740 Magnetospheric Physics: Magnetospheric configuration and dynamics; 2760 Magnetospheric Physics: Plasma convection; 2788 Magnetospheric Physics: Storms and substorms

1. Introduction

[2] Aboard the Imager for Magnetopause-to-Aurora Global Exploration (IMAGE) observatory, remote sensing of magnetospheric plasma dynamics is accomplished through photon, radio, and neutral atom based imaging [Burch et al., 2000]. Energetic ions in Earth's magnetosphere charge exchange with the extended neutral atmosphere to produce energetic neutral atoms (ENA) that are imaged by three different ENA cameras. The Low (LENA; [*Moore et al.*, 2000]), Medium (MENA; [*Pollock et al.*, 2000]), and High (HENA; [*Mitchell et al.*, 2000]) energy neutral imagers are sensitive to neutral atoms from 15 eV to 500 keV per nucleon.

[3] Charge exchange analysis of plasmas was originally developed as a means of measuring the ion temperature in thermonuclear fusion experiments [*Koidan*, 1971; *Afrosimov et al.*, 1975; *Scime and Hokin*, 1992]. The high density of modern fusion plasmas results in significant extinction of medium energy charge exchange neutrals as they move towards the edge of the plasma and intense emission of low energy neutral atoms from the outer edge of the plasma [*Scime et al.*, 1995]. Difficulties associated with analysis of optically thick media have forced laboratory plasma researchers to rely on complex modeling codes to interpret measured neutral energy spectra [*Burrell*, 1978]. In the magnetosphere, it is only very close to the Earth or at very low neutral energies that optical thickness of the medium becomes significant.

[4] In this work, we use ENA images obtained with the MENA instrument to construct the first remote measurements of ion temperature in the terrestrial magnetosphere. Given the energy range of the MENA imager for neutral hydrogen, 1–70 keV/nucleon, the neutral atom images include contributions from the ring current, plasma sheet, cusp, and their low altitude extensions. Above a few keV, the ring current is typically the brightest structure in the image. The MENA measurement process involves permitting the passage of collimated neutral flux to a microchannel plate detector while blocking the intense ultraviolet radiation reflected by the geocorona [*Gruntman*, 1991; *Scime et al*, 1994; *Balkey et al.*, 1998; *Pollock et al.*, 2000].

[5] For energetic neutral atom emission along a given viewing direction, the contribution to the high-energy portion of the energy spectrum (energies much greater than the ion temperature) is dominated by emission from the hottest region along the line of sight [*Scime and Hokin*, 1992]. The high-energy portion of the neutral atom energy spectrum, $F(E)$, generated via charge exchange collisions for a Maxwellian ion distribution of temperature T, is given by

$$F(E)dE \approx C\sigma(E)EdE\left[\frac{n_o(r)n_i(r)e^{-E/T(r)}}{\sqrt{2m_i\pi^3T(r)^3}}\right]_{r=x} e^{-\int_x^a \alpha(l)dl} \quad (1)$$

where $F(E)$ is in units of #/cm^2·s, C is a constant that accounts for the geometrical viewing properties of the instrument and the column line-of-sight integration over the hottest region (located at some point x along the line-of-sight). The hottest region is assumed to be of constant temperature and therefore the column integration of the neutral emission region yields a constant multiplicative factor. $T(x)$, $n_o(x)$, and $n_i(x)$ are the ion temperature, neutral density, and ion density at the same location, respectively. $\sigma(E)$ is the energy dependent charge exchange cross section between neutrals and ions of energy E [*Freeman and Jones*, 1974] and the integral over $\alpha(l)$ accounts for the reduction of neutral flux originating

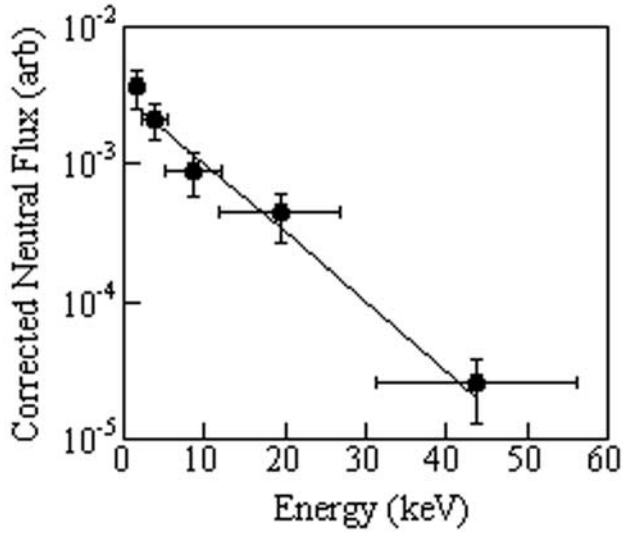

Figure 1. Logarithm of the corrected neutral atom flux versus neutral energy (filled circles) and a fit to the data using equation (2) (solid line). For these data, the best-fit ion temperature is 8.7 keV. The data come from a "green pixel" at +16° (along horizontal axis) and +32° (along vertical axis) in Figure 2a.

[1]West Virginia University, Morgantown, WV, USA.
[2]Southwest Research Institute, San Antonio, TX, USA.
[3]Los Alamos National Laboratory, Los Alamos, NM, USA.

0094-8276/02/2001GL013994$05.00

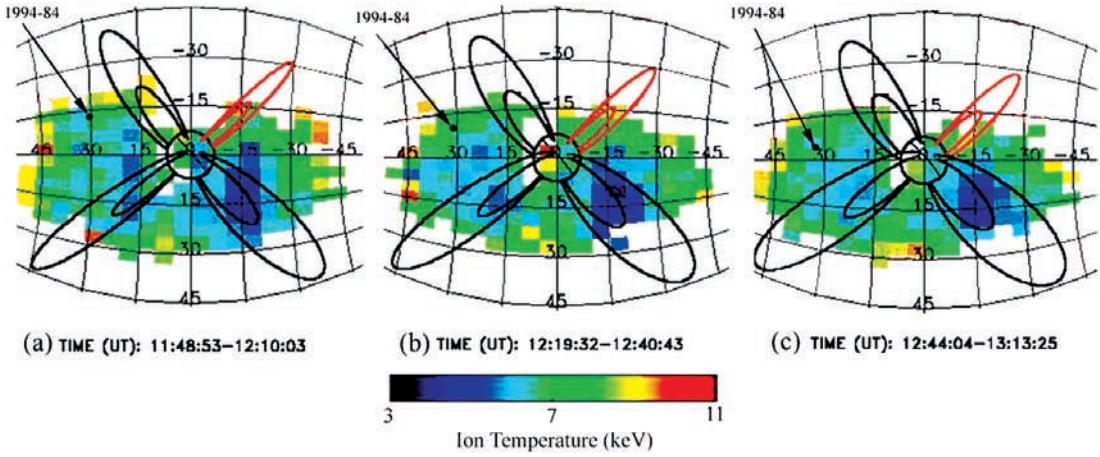

Figure 2. Twenty minute (10 spins of IMAGE) averaged ion temperature images from the MENA instrument on August 12, 2000. The black circle in the center of each image indicates Earth. Geomagnetic dipole field lines are shown at MLT = 6, 12, 18, and 24 hours and $L = 4$ and $L = 8$. The noon field lines are drawn in red and the grid pattern corresponds to the azimuthal and polar angles of the MENA instrument data bins. The solid black dot and line indicates the location of the 1994-84 MPA spacecraft at (a) 12:00 UT, (b) 12:30 UT, and (c) 13:00 UT.

from the location of the hottest region due to additional collisions or ionization as the neutrals travel from point x to the instrument located at point a [*Hutchinson*, 1987]. Outside of the plasmapause, the ion [*Kivelson and Russell*, 1995] and neutral densities [*Rairden et al.*, 1986] are low enough that the magnetosphere is optically thin to neutral atom emission. Thus,

$$\frac{F(E)dE}{\sigma(E)EdE} \approx C\left(\frac{n_o(x)n_i(x)}{\sqrt{2m_i\pi^3T(x)^3}}\right)e^{-E/T(x)}. \qquad (2)$$

Using equation (2), the peak ion temperature along the line-of-sight is determined from fits to the MENA energy spectra. The effective location of the measurement is where the right hand side of equation (2) is the largest for the range of energies measured. The absolute neutral and ion densities enter into equation (2) as constants and are not required for determination of the ion temperature. Since the energy spectrum decreases exponentially with energy, order of magnitude changes in the ion and neutral densities are overwhelmed by relatively modest differences in the ion temperature. Because background counts in the highest energy bins artificially raise the measured ion temperature, only image pixels with high count rates at all energies are used in this study.

[6] The above analysis assumes that the neutral atom fluxes are due to charge exchange between protons and neutral hydrogen. Since the five energy bins of the MENA instrument are based solely on time-of-flight measurements, the mass, and therefore the energy, of the neutral atoms is not known. Analysis of the distribution of detector pulse heights can, in principle, be used to separate oxygen atoms from hydrogen atoms in a statistical fashion, [*Pollock et al.*, 2000]. In this study, we assume that all of the measured fluxes are due to neutral hydrogen atoms. We also require counts in at least four energy bins before performing an ion temperature calculation.

2. Observations

[7] A typical ion energy spectrum (after correction for the charge exchange cross section and neutral energy) obtained from the MENA images during the August 12, 2000 storm is shown in Figure 1. Initial analysis of MENA images from this storm has been reported in a previous work [*Pollock et al.*, 2001]. The fit of equation (2) to the data yields an ion temperature of 8.7 keV. Note that the flux in lowest energy bin lies above the fitted curve. The low energy flux in the MENA data is consistently larger than what would be expected given the flux in the higher energy bins. This suggests that the source of the lower energy neutral flux has a larger spatial extent along the line-of-sight than the higher energy flux or that the low energy bins include contributions from higher mass neutrals such as oxygen.

[8] The remotely measured, magnetospheric ion temperature on August 12, 2000 is shown in Figure 2 at 12:00, 12:30 and 13:00

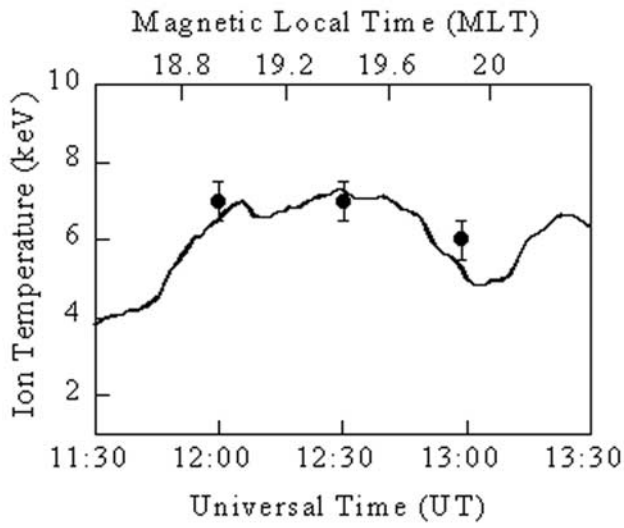

Figure 3. Total ion temperature versus time obtained from the 1994-84 MPA instrument (solid line) in geosynchronous orbit. Data have been smoothed with a twenty-minute boxcar average for consistency with the MENA image data. Remotely measured ion temperatures from MENA data (solid circles) with ±0.5 keV error bars at 12:00, 12:30, and 13:00 UT.

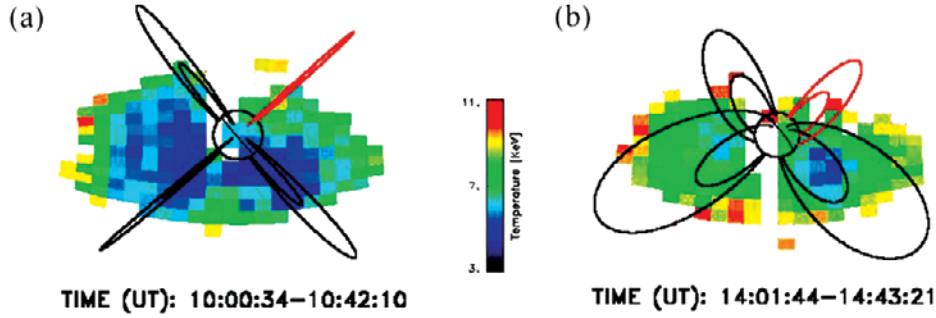

Figure 4. Forty minute (20 spins of IMAGE) averaged ion temperature images from the MENA instrument on August 12, 2000. Image format is the same as in Figure 3 except for the absence of the grid pattern. (a) At 10:20 UT, the ion temperatures on the dawn and dusk sides of the magnetosphere are similar. (b) At 14:20 UT, a strong asymmetry in the ion temperature is observed. For a small region on the dawn side, the ion temperatures are a factor of two smaller than on the dusk side.

(UT). The three ion temperature maps are based on twenty-minute averages (10 spins) of the neutral atom flux for comparison with the locally measured ion temperature at the location of the MPA 1994–84 spacecraft (Figure 3). The MPA measurements cover magnetic local times of 18:30 to 20:30. The MPA plasma instrument is a spherical section electrostatic energy analyzer that provides measurements of the ion and electron temperatures in geosynchronous orbit [*Bame et al.*, 1993]. On each of the three ion temperature images in Figure 2, a black arrow pointing to a solid black circle indicates the location, as seen from IMAGE, of the spacecraft carrying the MPA 1994–84 instrument. The MENA derived ion temperatures are also shown in Figure 3 for the times of the images in Figure 2. Both the absolute magnitude and temporal evolution of the MENA image based ion temperatures are consistent with the in-situ MPA measurements.

[9] These results demonstrate the need for the global information provided by IMAGE to place local measurements of plasma parameters in context. In this instance, MPA 1994–84 observes a locally measured decrease in ion temperature from 7 keV to 5 keV because it has moved into a region of the magnetosphere with a lower ion temperature, not because of an overall change in the ion temperature of the magnetosphere. In fact, the MENA images indicate that the ion temperature at the initial location of the spacecraft remains constant over the one-hour interval. For geosynchronous orbit, the half hour interval over which the ion temperature drops from 7 keV to 5 keV corresponds to a spatial scale of roughly 5,000 km.

[10] The remotely obtained MENA ion temperature maps can also provide unique information about magnetospheric structure and dynamics. It is clear in Figure 3 that around 12:00 UT during the August 12, 2000 storm, the dawn side of the magnetosphere is significantly cooler than the dusk side. Earlier in the day, the ion temperatures on the dawn and dusk sides were more similar (Figure 4a). As the day progressed, the asymmetry in ion temperature became more pronounced (Figure 4b). Although many of the storm intervals examined in this study yielded dawn-dusk symmetric ion temperature maps (such as Figure 4a), dawn-dusk asymmetry in the ion temperature, with the dawn side cooler than the dusk side, was consistently observed. Representative images of cooler dawn side ion temperatures are shown in Figure 5.

[11] Note that the images in Figure 4 and Figure 5 were obtained during different orientations of the IMAGE orbital plane relative to the Earth-Sun direction. Because the MENA instrument consists of three different imaging heads [*Pollock et al.*, 2000], errors in the relative calibrations of the heads could artificially create asymmetries of a few keV in the viewing direction perpendicular to the IMAGE orbital plane, i.e. left to right in the images. However the dawn-dusk asymmetries seen in Figure 4b and Figure 5c appear in lines-of-sight resolved by the spin of the IMAGE spacecraft, i.e. top to bottom in the images. Therefore, the lower dawn side ion

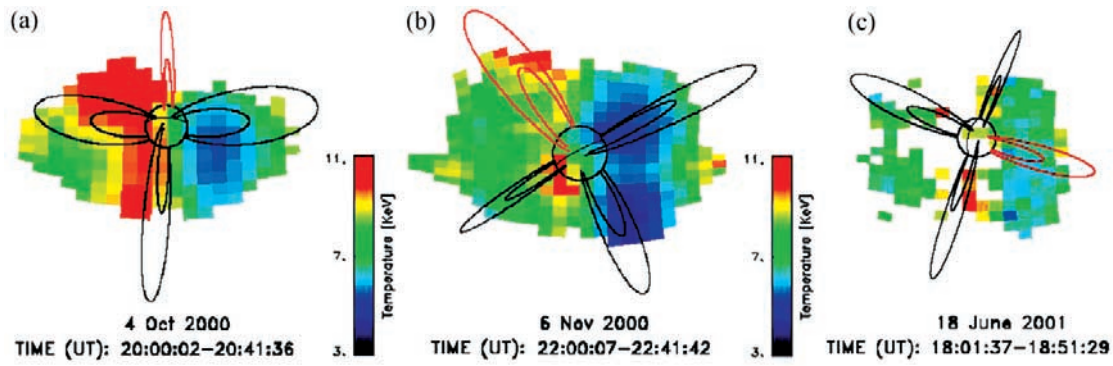

Figure 5. Three different storm time observations of dawn-dusk asymmetries in the remotely measured ion temperatures. The storms were chosen so that images for different orientations of the IMAGE orbital plane relative to the Sun-Earth line could be examined. (a) October 4, 2000 storm. (b) November 6, 2000 storm. (c) June 18, 2001 storm. The times over which the images were integrated are shown in each panel. The sparseness of the June 18, 2001 storm data is due to the weak nature of that storm.

temperatures appear to be geophysical in origin and not solely a result of instrumental effects.

3. Discussion

[12] These measurements demonstrate that, without complex inverse modeling, the high-energy portion of the neutral atom emission observed by the MENA instrument aboard IMAGE can be used to remotely determine the local ion temperature at the hottest place along each line of sight passing through the magnetosphere. Given the qualitative and quantitative agreement with the MPA measurements, the remote MENA ion temperatures appear to correspond to the local ion temperatures in the equatorial plane.

[13] During storm intervals, a dawn-dusk asymmetry is often observed in the ion temperature images with the dawn side of the magnetosphere being cooler than the dusk side. Similar asymmetries in the ring current ion temperatures during storm times have been reported from in-situ measurements [*Studemann et al.*, 1987]. Hints of a storm time dawn-dusk asymmetry in energetic neutral atom fluxes were also suggested in a modeling study of neutral atom emission observed by ISEE 1 [*Roelof*, 1987]. In-situ measurements of ring current evolution during geomagnetic storms suggest a number of possible explanations for the asymmetry. One possibility is that competition between magnetic drifts (gradient and curvature) and *E x B* drifts limits convection of high-energy ions from the night side plasma sheet [*Ejiri et al.*, 1980]. Unfortunately, the coarseness of the MENA energy bins and poor counting statistics at high energy make it difficult to determine if there is a distinct high-energy cutoff in the neutral energy spectrum on the dawn side. Another possibility is that ion energy conservation in the dawn to dusk electric field could explain the lower average energy of the ions on the dawn side [*Ebihara et al.*, 1999]. Further studies are planned to determine which mechanism, if either, can be confirmed through analysis of individual energy spectra.

[14] These initial imaging results demonstrate how global measurements can help distinguish between temporal and spatial effects in single point, in-situ plasma measurements. By integrating over long time intervals or by constructing more sensitive neutral atom imagers, it may also be possible to use remote measurements of ion temperature to identify regions of wave-driven ion heating near the magnetopause or in the magnetotail.

[15] **Acknowledgments.** This work was supported at SWRI and WVU under NASA contract NAS5-96020. The Los Alamos portion of this work was conducted under the auspices of the U.S. Department of Energy.

References

Afrosimov, V. V., E. L. Berezovskii, I. P. Gladkovskii, A. I. Kislyakov, M. P. Petrov, and V. A. Sadovnikov, Multichannel energy and mass analyzer for atomic particles, *Sov. Phys. Tech. Phys.*, *20*, 33, 1975.

Balkey, M. M., E. E. Scime, M. L. Schattenburg, and J. van Beek, Effects of Slit Width on VUV Transmission Through Sub-Micron Period, Free-Standing, Transmission Gratings, *App. Optics*, *37*, 5087, 1998.

Bame, S. J., D. J. McComas, M. F. Thomsen, B. L. Barraclough, R. C. Elphic, J. P. Glore, J. T. Gosling, J. C. Chavez, E. P. Evans, and F. J. Wymer, Magnetospheric plasma analyzer for spacecraft with constrained resources, *Rev. Sci. Instrum.*, *64*, 1026, 1993.

Burrell, K. H., NEUCG: A Transport Code for Hydrogen Atoms in Cylindrical Hydrogenic Plasmas, *J. Comp. Physics*, *27*, 88, 1978.

Ebihara, Y., S. Barabash, and M. Ejiri, On the global production rates of energetic neutral atoms (ENAs) and their association with the Dst index, *Geophys. Res. Lett.*, *26*, 2929, 1999.

Ejiri, M., R. A. Hoffman, and P. H. Smith, Energetic particle penetrations into the inner magnetosphere, *J. Geophys. Res.*, *85*, 653, 1980.

Freeman, R. L., and E. M. Jones, Atomic Collision Processes in Plasma Physics Experiments, *Culham Laboratory Report CLM-R*, *137*, 1, 1974.

Gruntman, M. A., Submicron structures: promising filters in VUV—a review, in *VUV, X-Ray, and Gamma-Ray Instrumentation for Astronomy*, edited by O. H. Siegmund and R. E. Rothschild, *Proc. SPIE, 1549*, 385, 1991.

Hutchinson, I. H., *Principles of Plasma Diagnostics*, pp. 284–302, Cambridge University Press, Cambridge, 1987.

Kivelson, M., and C. T. Russell, *Introduction to Space Physics*, pp. 239, Cambridge University Press, New York, 1995.

Koidan, V. S., Multichannel Energy Analysis of Ions and Fast Charge-Exchange Atoms in the Investigation of a High Temperature Plasma, *Sov. Tech. Phys.*, *3*, 63, 1971.

Mitchell, D. G., et al., High Energy Neutral Atom (HENA) imager for the IMAGE mission, *Space Sci. Rev.*, *91*, 67–112, 2000.

Moore, T. E., et al., The Low Energy Neutral Atom imager for IMAGE, *Space Sci. Rev.*, *91*, 155–195, 2000.

Pollock, C. J., et al., Medium Energy Neutral Atom (MENA) imager for the IMAGE Mission, *Space Sci. Rev.*, *91*, 113–154, 2000.

Pollock, C. J., et al., First Medium Energy Neutral Atom (MENA) Images of Earth's Magnetosphere during Substorm and Storm-time, *Geophys. Res. Lett.*, *28*, 1147, 2001.

Rairden, R. L., L. A. Frank, and J. D. Craven, Geocoronal Imaging With Dynamics Explorer, *J. Geophys. Res.*, *91*, 13,613, 1986.

Scime, E. E., and S. Hokin, Design and calibration of a fast time resolution charge exchange analyzer, *Rev. Sci. Instrum.*, *63*, 4527, 1992.

Scime, E. E., H. O. Funsten, M. Gruntman, and D. J. McComas, A Novel Low Energy Neutral Atom Imaging Technique, *Opt. Eng.*, *33*, 357, 1994.

Scime, E. E., H. O. Funsten, and D. J. McComas, Three dimensional neutral atom imaging of tokamak plasmas, *Rev. Sci. Instrum.*, *66*, 336, 1995.

Studemann, W., B. Wilken, G. Kremser, A. Korth, J. F. Fennell, B. Blake, R. Koga, D. Hall, D. Bryant, F. Soraas, K. Bronstad, T. A. Fritz, R. Lundin, and G. Gloeckler, The May 2–3, 1986 magnetic storm: first energetic ion composition observations with the MICS instrument on Viking, *Geophys. Res. Lett*, *14*, 455, 1987.

E. Scime, A. M. Keesee, and J. L. Kline, West Virginia University Morgantown, WV 26506, USA. (escime@wvu.edu; asmith38@wvu.edu; jkline2@wvu.edu)

J.-M. Jahn, and C. J. Pollock, Southwest Research Institute, San Antonio, TX 78238, USA. (jjahn@swri.org; cpollock@swri.edu)

M. Thomsen, Los Alamos National Laboratory, Los Alamos, NM 87545, USA. (mthomsen@lanl.gov)